How patchy can one get and still condense? The role of dissimilar patches in the interactions of colloidal particles

Jose Maria Tavares, Paulo Ivo Teixeira, Margarida Telo da Gama

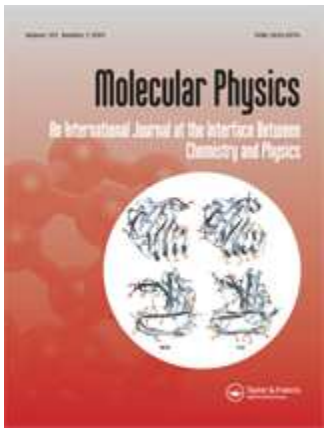

How patchy can one get and still condense? The role of dissimilar patches in the interactions of colloidal particles

Journal:	*Molecular Physics*
Manuscript ID:	TMPH-2008-0441.R1
Manuscript Type:	Special Issue Paper - Dr. Jean-Jacques Weis
Date Submitted by the Author:	24-Feb-2009
Complete List of Authors:	Tavares, Jose; Instituto Superior de Engenharia de Lisboa, Centro de Fisica Teorica e Computacional Teixeira, Paulo; Instituto Superior de Engenharia de Lisboa, Centro de Fisica Teorica e Computacional Telo da Gama, Margarida; Universidade de Lisboa, Centro de Fisica Teorica e Computacional
Keywords:	patchy colloids, phase diagram, critical point
Note: The following files were submitted by the author for peer review, but cannot be converted to PDF. You must view these files (e.g. movies) online.	
TMPH-2008-0441.R1.zip	

How patchy can one get and still condense? The role of dissimilar patches in the interactions of colloidal particles

J. M. Tavares[1,2], P. I. C. Teixeira[1,2] and M. M. Telo da Gama[2,3]

[1]*Instituto Superior de Engenharia de Lisboa*

Rua Conselheiro Emídio Navarro 1, P-1950-062 Lisbon, Portugal

[2]*Centro de Física Teórica e Computacional da Universidade de Lisboa*

Avenida Professor Gama Pinto 2, P-1649-003 Lisbon, Portugal

[3]*Departamento de Física, Faculdade de Ciências da Universidade de Lisboa*

Campo Grande, P-1749-016 Lisbon, Portugal

(Dated: 13 February 2009)

Abstract

We investigate the influence of strong directional, or bonding, interactions on the phase diagram of complex fluids, and in particular on the liquid-vapour critical point. To this end we revisit a simple model and theory for associating fluids which consists of spherical particles having a hard-core repulsion, complemented by three short-ranged attractive sites on the surface (sticky spots). Two of the spots are of type A and one is of type B; the interactions between each pair of spots have strengths ϵ_{AA}, ϵ_{BB} and ϵ_{AB}. The theory is applied over the whole range of bonding strengths and results are interpreted in terms of the equilibrium cluster structures of the coexisting phases. In systems where unlike sites do not interact (i.e., where $\epsilon_{AB} = 0$), the critical point exists all the way to $\epsilon_{BB}/\epsilon_{AA} = 0$. By contrast, when $\epsilon_{BB} = 0$, there is no critical point below a certain finite value of $\epsilon_{AB}/\epsilon_{AA}$. These somewhat surprising results are rationalised in terms of the different network structures of the two systems: two long AA chains are linked by one BB bond (X-junction) in the former case, and by one AB bond (Y-junction) in the latter. The vapour-liquid transition may then be viewed as the condensation of these junctions and, we find that X-junctions condense for any attractive ϵ_{BB} (i.e., for any fraction of BB bonds), whereas condensation of the Y-junctions requires that ϵ_{AB} be above a finite threshold (i.e., there must be a finite fraction of AB bonds).

PACS numbers: 64.70.F-, 64.75.Yz, 61.20.Qg

I. INTRODUCTION

It is a pleasure, and a great honour, to contribute to J. J. Weis' Fest. Although the earliest paper by JJ that most of us know of is the celebrated 1972 Verlet-Weis 'Equilibrium Theory of Simple Liquids' [1], our collaboration did not start until about 20 years later. The problem that we tackled may be related to that of the 1972 paper in the sense that it concerns the understanding of what was thought until then to be a simple liquid. The structure of strongly dipolar fluids was, however, revealed in a seminal paper of JJ (in collaboration with D. Levesque) [2] to be strikingly different from that of simple fluids. We may say, without exageration, that the structure and phase diagram of strongly dipolar fluids have resisted a complete understanding, despite the large number of papers written on the subject over the past 15 years. We will not attempt to give an up-to-date review of the problem here, but shall restrict ourselves to describing it, in the light of JJ's contributions and of the impact of these contributions on our work, the outcome of a fruitful collaboration that will always be remembered. We shall then proceed to discuss recent developments on a different problem that we hope will shed light on dipolar fluid behaviour, and present our first contribution along these lines, which we would like to dedicate to JJ.

The condensation of simple fluids is driven by the free energy balance between the high-entropy gas and the low-energy liquid phases. This transition appears to be generic in simple fluids interacting via isotropic intermolecular potentials that comprise a short-ranged repulsion and a longer-ranged attraction. The dipolar hard- or soft-sphere (DHS or DSS) fluid is a model in which hard or soft spheres with an embedded central point dipole interact through the dipole-dipole potential. As the isotropic effective interaction between two dipoles (obtained by taking the logarithm of the angle-averaged Boltzmann factor of the dipole-dipole potential) is attractive, one may anticipate phase behaviour analogous to that of simple fluids. Indeed, a recent calculation of the free energy of the DHS at several temperatures, based on Monte Carlo (MC) simulations [3], suggests the presence of an isotropic fluid-fluid transition at low densities, lending some support to the analogy with simple fluids. However, the structure of DHS at low densities, where the transition has been reported, is dramatically different from that of isotropic fluids. Numerical simulations of DHS [2] and also of Stockmayer fluids [4] for dipolar interaction strengths of the order of the thermal energy, have shown that the anisotropy of the dipolar potential promotes the formation of

self-assembled aggregates (chains, rings and more complex clusters), in sharp contrast with the isotropic compact clusters observed in simple fluids. Moreover, unlike in simple fluids the pair correlation function of DHS is strongly peaked at contact and the internal energy is nearly independent of the density [3]. It is unclear whether strong association precludes any kind of fluid-fluid phase separation, as failure to observe it may be an artifact of the simulation techniques. The situation in these and related dipolar fluid simulations [5–7] remains controversial, requiring the development of new methods [8] to review the dipolar condensation problem in the light of recent theoretical results.

In parallel, there is an urgent need to develop analytical treatments of strongly correlated dipolar systems. Association theories [9–13] that include the effect of cluster formation in the thermodynamics, reproduce rather well the slow variation of the internal energy with the density and the cluster size (or mass) distribution. The simplest of these theoretical approaches, built on the basis of simulation results, assumes that the only effect of the dipolar interaction is to drive cluster formation and hence describes the DHS fluid as an ideal mixture of self-assembling clusters. However, these theories fail to predict the existence of phase transitions unless direct or indirect interactions between the clusters are added. In collaboration with JJ [12, 14] we identified various types of clusters in a quasi two-dimensional (2D) DHS fluid: chains, rings and defect clusters, the last named henceforth referred to as networks, as in Safran *et al.*'s work [15–17]. The dipolar chains and rings at very low densities were fully characterised by analysing their conformational properties, internal energy and size (or mass) distribution, revealing a strong analogy with equilibrium polymers [18]. Still, we did not address the question of liquid-vapour coexistence due to the difficulty in extending the analysis to networks. Somewhat later we found a way of including the effect of network formation in the theory, which allowed us to conclude that the simulation results support the presence of a phase transition in quasi-2D DHSs [19]. Although we did not perform a quantitative comparison with the theory put forward by Tlusty and Safran [15], we noted that the mechanism for condensation proposed by these authors, based on not only the density difference between the coexisting phases, but also on the topologies of the aggregates in either phase, was the same as that described in [19]. The low-density chain-like phase is characterised by a large number of 'end' defects – particles at the ends of chains with only one neighbour – whereas the high-density 'network' phase is rich in chains with branching points – particles with three (Y-junctions) or more neighbours

(X-junctions in the case of four neighbours).

Alternative treatments of the competition between phase separation and association in the Stockmayer and DHS fluid include variants of the Flory-Huggins (FH) model of equilibrium polymerisation [20, 21] and a thermodynamic perturbation theory for associating fluids [22]. The former rely on casting the free energy of the Stockmayer fluid in FH form, while the latter, though apparently quite accurate [22, 23] is substantially more difficult to implement than Wertheim's association theory [24, 25] that will be discussed in the next section.

A related line of work concerns the novel type of soft matter known as associating colloids. Unlike in atomic systems, we are now able to control the interactions between colloidal particles, thus opening up the possibility of new structural and thermodynamic behaviour [26]. Of particular interest are the so-called patchy colloids, the surfaces of which are patterned so that they attract each other via discrete 'sticky spots' of tunable number, size and strength. Besides their relevance to applications or in biological systems (e.g., protein solutions), patchy colloids have important connections with notoriously difficult classical liquids such as water and strongly dipolar fluids [27]. An understanding of these novel systems will therefore shed light on more traditional forms of liquid matter. In particular, we note that understanding the nature of the dipolar fluid phase transitions is important for applications based on dispersions of ferromagnetic nanoparticles [28–30], where strong dipolar interactions are present, as well as for fundamental reasons. In fact, the interplay between cluster formation and condensation is a general problem, relevant in a variety of other theoretical contexts.

Our ultimate purpose is to develop and study a model that retains the essential symmetry of dipolar forces that leads to association, while leaving out features believed to be inessential, such as their long range and complex angular dependence. As a first step, following pioneering work by Sciortino and co-workers [31–33], we applied Wertheim's theory, as formulated by Jackson *et al.* [34], to patchy particles decorated with three interaction sites: two of type A, whose interaction strength ϵ_{AA} sets the energy scale, and one of type B and strength ϵ_{BB}. Unlike sites also interact, with strength ϵ_{AB}.

When $\epsilon_{BB} = \epsilon_{AB} = 0$ we recover the limit of two identical patches of strength ϵ_{AA} [31–33]. However, this limit turns out to be quite subtle: in systems where unlike sites do not interact (i.e., where $\epsilon_{AB} = 0$), the critical point exists all the way to $\epsilon_{BB}/\epsilon_{AA} = 0$. By contrast, when $\epsilon_{BB} = 0$, there is no critical point below a certain finite value of $\epsilon_{AB}/\epsilon_{AA}$. These somewhat

surprising results can be rationalised in terms of the different network structures of the systems: two long AA chains are linked by one BB bond (X-junction) in the former case, and by one AB bond (Y-junction) in the latter. The vapour-liquid transition may then be viewed as the condensation of these junctions, and we find that X-junctions condense for any strength of the BB attraction (i.e., for any fraction of BB bonds) whereas condensation of the Y-junctions requires that the AB interaction strength be above a finite threshold (i.e., there must be a finite fraction of AB bonds), in line with previous work [16].

This paper is organized as follows: in section II we provide a derivation of the theory and apply it to the model with three different interaction patches. In section III we present our results for the phase diagrams and critical points. These are further discussed in section IV, where we summarise our conclusions. A number of technical details are given in an appendix.

II. THEORY AND MODEL

We consider a system of N hard spheres (HSs) of diameter σ and volume $v_s = (\pi/6)\sigma^3$, each decorated with three bonding sites (or sticky spots) on their surface. Two of these spots are identical, and labelled A, while the third is different, and labelled B. In general, two spheres may form bonds of types AA, BB or AB. Each bond corresponds to a short-ranged attractive interaction between two bonding sites, which is treated as a perturbation of the HS potential. We assume that these potentials are square wells, with depths ϵ_{ij} (where $i, j = A, B$), and their ranges are chosen so that each bonding site can only take part in one bond. The positions of the bonding sites over the surface of the sphere are such that it is not possible to have more than one bond between two spheres.

The above requirements are introduced to satisfy the assumptions made in Wertheim's theory, which then provides a general expression for the contribution of bonds to the free energy, F_b. Wertheim's derivation is based on a re-summed cluster expansion, where the significance of each of the approximations is mathematically well understood [24, 25]. The results are, however, rather formal and have been reformulated by Jackson *et al.* [34] in a more convenient form that will be used here. An analysis of Wertheim's theory in the fully bonded limit reveals that it approximates (i) F_b by its low-density limit; and (ii) the $n-$body correlation function by a superposition of pair (two-body) correlation functions of the

reference system [35].

For the present model, a fluid of identical spheres with two A and one B bonding sites, the bonding free energy, F_b, is given by [34],

$$\beta f_b \equiv \frac{\beta F_b}{N} = 2\ln X_A + \ln X_B - X_A - \frac{X_B}{2} + \frac{3}{2}, \tag{1}$$

where $\beta \equiv 1/(k_{\rm B}T)$, T is the temperature, $k_{\rm B}$ is the Boltzmann constant, and X_i is the probability of having a sticky spot of type i *not* bonded. $1 - X_i$ is thus the fraction of bonding sites of type i that do take part in bonds. The variables X_i are related to the density and temperature through the law of mass action that is obtained by treating bond formation as a chemical reaction. We recall that this is equivalent to disregarding loops in the branched clusters, preserving only pair correlations [36]. Clusters consist of uncorrelated bonds; longer-range correlations, including intracluster self-avoidance, are neglected. The inter-cluster excluded volume is taken into account through the reference fluid entropic term.

The law of mass action then yields the following two equations [24, 25, 34]:

$$X_A + 2\eta\Delta_{AA}X_A^2 + \eta\Delta_{AB}X_AX_B = 1, \tag{2}$$

$$X_B + \eta\Delta_{BB}X_B^2 + 2\eta\Delta_{AB}X_AX_B = 1, \tag{3}$$

where $\eta \equiv (N/V)v_s$ is the packing fraction, and,

$$\Delta_{ij} = \frac{1}{v_s}\int_{v_{ij}} g_{ref}(\mathbf{r})\left[\exp(\beta\epsilon_{ij}) - 1\right] d\mathbf{r}. \tag{4}$$

This integral is calculated over v_{ij}, the volume of bond ij, and g_{ref} is the pair correlation function (PCF) of the reference system. $M_iM_j\Delta_{ij}/(1+\delta_{ij})$ (with $M_A = 2$ and $M_B = 1$ the numbers of A and B sites per particle and δ_{ij} the Kronecker delta) plays the role of the equilibrium constant for the reaction between sites i and j [37].

Here we shall take all bonds to have the same volume, $v_{ij} = v_b$. The reference system is chosen to be the HS fluid, and the low-density (ideal gas) approximation for the PCF, $g_{ref}(\mathbf{r}) = 1$, will be used. Within these two approximations, equation (4) becomes

$$\Delta_{ij} = \frac{v_b}{v_s}\left[\exp(\beta\epsilon_{ij}) - 1\right]. \tag{5}$$

The free energy per particle is, therefore,

$$\beta f = \beta f_{HS} + \beta f_b, \tag{6}$$

which is a function of (η, T) only. In what follows we shall use the Carnahan-Starling approximation for f_{HS} [38]; X_A and X_B are obtained by solving equations (2) and (3) for fixed (η, T). Because Wertheim's theory treats all bonds independently, it does not provide any direct information on the geometry of the resulting aggregates. We can nevertheless infer what the lowest-energy structures (without any loops, see above) are in the limiting cases where two of the three ϵ_{ij} go to zero (see figure 1): chains ($\epsilon_{AB} = \epsilon_{BB} = 0$, $\epsilon_{AA} \neq 0$); dimers ($\epsilon_{AA} = \epsilon_{AB} = 0$, $\epsilon_{BB} \neq 0$) and hyperbranched polymers ($\epsilon_{AA} = \epsilon_{BB} = 0$, $\epsilon_{AB} \neq 0$). We can also infer what structures will appear when we perturb the pure AA-chain limit: two chains can attach at an X-junction (BB bond, figure 2a) or at a Y-junction (AB bond, figure 2b).

We shall focus on the interplay between self-assembly and condensation in the context of the present model, a number of special cases of which have been considered previously. The case $\epsilon_{ij} = \epsilon$ (i.e., each sphere has three identical bonding sites) was extensively studied in [31, 33], by comparing simulations to Wertheim's theory: agreement for the phase diagrams was excellent. Furthermore, it was established that the number of bonding sites per particle, M, is the key parameter controlling the location of the liquid-vapour critical point: on decreasing M, this moves towards ever lower densities and temperatures, such that liquid-vapour coexistence ceases to exist if $M \leq 2$ [31–33]. Simulation and theory also provide evidence that, for mixtures of particles with two and three identical sticky spots, the average number $\langle M \rangle$ of bonding sites per particle can be varied continuously by changing the concentration of the two species, and the critical point may be made to approach zero density and temperature continuously, as $\langle M \rangle \to 2$ [31]. This makes it possible to realise equilibrium liquid states with arbitrarily low density (empty liquids), which would be unfeasible with spherically symmetric interaction potentials.

In the case $\epsilon_{AA} = \epsilon_{AB} = 0$ [34], only dimer formation is allowed and there is no condensation. Finally, in the case $\epsilon_{AB} = \epsilon_{BB} = 0$ only linear self-assembly is allowed: no critical point exists [31, 33, 37], and one expects a polymerisation transition to occur when $T \to 0$ [39]. The detailed fashion in which the critical temperature vanishes as the bonding energies, ϵ_{AB} and ϵ_{BB}, decrease towards zero depends on the order in which the limits $\epsilon_{AB} \to 0$ and $\epsilon_{BB} \to 0$ are taken, which in turn determines the type of network that is formed, as we shall discuss in the following sections.

As a final remark before presenting our results, we recall that, as the monomer density

is increased or the temperature decreased, these systems will pass through a percolation threshold, where a network spanning the entire volume is formed. This transition is purely topological, and has no thermodynamic signature, unlike the condensation described below. The percolation transition and the correlation between the structural and thermodynamic properties of this class of associating fluids will be addressed in future work.

III. RESULTS

A. The phase diagram

We have found the phase diagram by equating the pressures and chemical potentials of the coexisting liquid and vapour phases, given by equations (21) and (24), and solving these, together with the mass-action law equations (2) and (3) for the two phases.

The resulting set of six coupled non-linear equations was solved numerically using NETLIB routine HYBRD. For consistency with Sciortino *et al.*'s work, we set $v_b = 0.000332285\sigma^3$. Likewise we introduce the reduced density $\rho^* = (N/V)\sigma^3 = \eta/v_s$, reduced temperature $T^* = k_{\mathrm{B}}T/\epsilon_{AA}$, and reduced interaction strengths $\epsilon^*_{BB} = \epsilon_{BB}/\epsilon_{AA}$, $\epsilon^*_{AB} = \epsilon_{AB}/\epsilon_{AA}$. This amounts to taking σ, the HS diameter, as our unit of length, and ϵ_{AA} as our unit of energy. Note that this choice of energy scale is neutral from the point of view of criticality, as AA bonds can only lead to chaining, and not phase coexistence, at any finite temperature.

Figure 3 shows phase diagrams for $\epsilon^*_{BB} = 1$ and variable ϵ^*_{AB}. For $\epsilon^*_{AA} = \epsilon^*_{AB} = 1$ this differs slightly from Sciortino *et al.*'s result [31, 33] for colloids with $M = 3$ identical spots, because those authors used a more sophisticated approximation for the PCF. However, like them we also find that the liquid phase has a rather low density, especially when ϵ^*_{AB} is small. As expected, the liquid phase is more extensively bonded, i.e., X_A and X_B, the fractions of unbonded A and B sites, respectively, are smaller in the liquid than in the vapour.

Weakening the AB bond shrinks the region of two-phase coexistence (figure 3a), as fewer AB bonds form in the liquid phase and more in the vapour phase (figures 3b and 3c). However, in the limit of no AB bonds ($\epsilon^*_{AB} = 0$) we still get condensation, driven exclusively by the presence of BB bonds: chains formed by AA bonds are linked through BB bonds in a way reminiscent of the fourfold or X-junctions defined in [15–17] (see figure 2a). The

two phases differ in the number and sizes of these chain aggregates, with $X_B \lesssim X_A$ in either phase.

If, on the other hand, the AB bond is strengthened, the critical temperature T_c^* first goes up and then saturates, while the critical density ρ_c^* first goes through a maximum and then approaches zero. This corresponds to AB bonds being formed in preference to BB bonds. An AB bond is a linkage between an interior particle of one chain and the end of another chain: two AA chains are linked through an AB bond, reminiscent of the Y-junctions defined in [15–17] (see Figure 2b). Clearly, increasing ϵ_{AB}^* favours the assembly of Y-junctions, leading to less compact aggregates than do X-junctions, hence a lower density. In the limit of large ϵ_{AB}^* there is complete association of the B sites at the critical point, leading to $X_B \to 0$ and $X_A \to 0.5$ because there are only half as many B sites as there are A, sites, as can be seen from figures 3b and 3c. This is consistent with the formation of highly ramified clusters akin to hyperbranched polymers [40], the size of which grows as the bond gets stronger.

This behaviour of the critical density is similar to that observed experimentally for long n-alkanes [41–43], where novel techniques revealed that the critical mass density reaches a maximum and then starts to decrease as the chain length increases [41]. Simulation results [44–46] give support to this finding

Note that although Wertheim's theory was originally developed to treat fluids of associating HSs, it yields, in the limit of infinite association strength, a polydisperse polymer mixture [47]. By invoking the polymer-solvent analogy, it is expected from Flory-Huggins theory that the pure polymer fluid should reach an asymptotic critical temperature, whereas the critical mass density should become vanishingly small, as the chain length goes to infinity. This is corroborated by renormalisation group calculations [48, 49], which also show that the corrections to scaling are large for chain lengths that occur in experiments [50]. When self-assembly is involved, the way in which the infinite chain limit is attained could be even more complicated. However, polydispersity is irrelevant at the critical point and the results of figure 3 confirm that the same type of critical behaviour occurs in associating systems.

Figure 4 shows phase diagrams for $\epsilon_{AB}^* = 0.75$ and variable ϵ_{BB}^* (effects are qualitativeley the same for $\epsilon_{AB}^* = 1$, only less pronounced). Again the liquid phase has quite low densities, especially when $\epsilon_{BB}^* \ll 1$. The critical point saturates at both large and small BB bond

strengths (i.e., it changes very little with ϵ^*_{BB} in the limits of both small and large ϵ^*_{BB}, as can be seen from figures 5a and 5b), but ρ^*_c goes to zero in neither limit. Increasing ϵ^*_{BB} broadens the region of two-phase coexistence as it permits more and more compact clusters through X-junction formation (figure 4a). In the limit of large ϵ^*_{BB} there is thus a high degree of association of B sites (X_B is small) in either phase (figure 4c), whereas A sites are fairly strongly associated (X_A is fairly small) in the liquid phase, but rather more weakly associated (X_A is large) in the vapour phase (figure 4b). This suggests that the vapour phase should consist mostly of BB dimers, and the liquid phase of BB dimers connected by AA bonds.

On the other hand, as $\epsilon^*_{BB} \to 0$, A-site association is almost complete ($X_A \approx 0$) in the liquid phase, and fairly strong ($X_A \leq 0.45$) in the vapour phase (figure 4b). At the same time, there are few bonded B sites (X_B is large) in the vapour phase, and not so many in the vapour phase (figure 4c). This implies that most A sites are bonded to other A sites, forming chains in both phases, but that more A sites are bonded to B sites, forming Y-junctions, in the liquid phase than in the vapour phase. These AB bonds are enough to sustain the critical point.

B. The critical point

It should be obvious by now that we have a rich parameter space to explore, as both ϵ^*_{BB} and ϵ^*_{AB} can be varied independently. In this paper we therefore chose to concentrate on the approach to the already known limit $\epsilon_{AB} = \epsilon_{BB} = 0$, where no liquid-vapour critical point exists. We ask ourselves: how exactly does the critical point vanish?

The critical point is found by equating to zero the first and second derivatives of the pressure with respect to the density. This calculation is described in detail in the Appendix. Figures 5 and 6 show the critical density ρ^*_c, critical temperature T^*_c, fraction of unbonded A sites at the critical point X_{Ac} and fraction of unbonded B sites at the critical point X_{Bc}, as ϵ^*_{BB} and ϵ^*_{AB} go to zero along two different routes: $\epsilon^*_{BB} \to 0$ and fixed ϵ^*_{AB} (figure 5); $\epsilon^*_{AB} \to 0$ and fixed ϵ^*_{BB} (figure 6).

Let us consider the first of these routes (figure 5). Taking a section at constant ϵ^*_{BB}, T^*_c decreases with ϵ^*_{AB} (see figure 5b). By contrast, ρ^*_c exhibits a rather complex non-monotonic dependence on ϵ^*_{AB} when $\epsilon^*_{BB} \lesssim 2$ (see figure 5a): it increases with decreasing ϵ^*_{AB} up to

$\epsilon^*_{AB} \approx 1$, below which it decreases, reaching extremely small values even for $\epsilon^*_{AB} = 0.5$. This behaviour can be rationalised as follows:

- If $\epsilon^*_{AB} \gg 1$, most bonds are AB with a few AAs ($X_B \ll 1$ and $X_A \approx 0.5$, see figures 5c and 5b): we are in the hyperbranched cluster limit and the critical density is low.
- If $\epsilon^*_{AB} \approx 1$, all bonds have approximately the same strength, similarly to [31, 33].
- Finally if $\epsilon^*_{AB} < 1$ we have mostly AA bonds ($X_A \ll 1$ and $X_B \approx 1$, see figures 5c and 5d), hence chains, connected by a few AB bonds (Y-junctions): the number of BB bonds drops as $\epsilon^*_{BB} \to 0$, the critical clusters are expected to be large and the critical density low.

Now the second route (figure 6). Taking a section at constant ϵ^*_{AB}, T_c decresases as ϵ^*_{BB} decreases (see figure 6b). Three regimes can be identified, in terms of the dominant structures:

- If $\epsilon^*_{AB} \gg 1$, we are again in the hyperbranched cluster limit and ρ^*_c is low (see figure 6a): most bonds are AB with a few AAs ($X_B \ll 1$ and $X_A \approx 0.5$, see figures 6d and 6c).
- If $\epsilon^*_{AB} \approx \epsilon^*_{BB} \approx 1$, we are close to three identical bonding sites behaviour and ρ^*_c has a maximum (see figure 6a); the extent of both A- and B-site bonding is moderate (though not small, see figures 6c and 6d), which suggests that the critical clusters are not too large.
- If $\epsilon^*_{AB} \ll 1$ and ϵ^*_{BB} is not too small, ρ^*_c first decreases with decreasing ϵ^*_{BB}, up to about $\epsilon^*_{BB} \approx 1$, below which it decreases (see figure 6a). For $\epsilon^*_{BB} \geq 0.75$, ρ^*_c stays close to its maximum, so the critical clusters are probably relatively small. However for $\epsilon^*_{BB} \lesssim 0.5$ there is a dramatic change: ρ^*_c drops to very small values, most A sites are bonded (X_A gets very small, see figure 6c) but hardly any B sites ($X_B \approx 1$, see figure 6d). Both phases consist mostly of AA-bonded chains with some residual AB and BB attractions.

We ran into numerical problems (failure to converge to a solution of the set of non-linear equations) whenever both ϵ^*_{BB} and ϵ^*_{AB} are small: these can be traced to the extremely low

value of the critical density discussed above. We therefore investigated this limit analytically. Start by noting that, in the limit of purely linear self-assembly, $\epsilon^*_{BB} = \epsilon^*_{AB} = 0$ and equation (3) gives $X_B = 1$ (no bonding of B sites). Moreover, equation (2) reduces to

$$X_A + 2\eta\Delta_{AA}X_A^2 = 1. \tag{7}$$

In the limit $T^* \ll 1$, we have $\Delta_{AA} \gg 1$ and $X_A \ll 1$ (complete association of A sites), so equation (3) becomes

$$X_A = \frac{1}{(2\Delta_{AA}\eta)^{1/2}}. \tag{8}$$

The two cases of interest were treated as perturbations to this limit.

1. X-junction driven criticality: $\epsilon^*_{AB} = 0$, $\epsilon^*_{BB} \to 0$

When $\epsilon^*_{AB} = 0$, equation (3) becomes,

$$X_B + \eta\Delta_{BB}X_B^2 = 1. \tag{9}$$

In the limit $\epsilon^*_{BB} \ll 1$, we must have $X_B \approx 1$ (i.e., no B sites are bonded), and consequently $\eta\Delta_{BB} \approx 0$. Therefore, in this limit, equation (9) can be approximated by

$$X_B = 1 - \eta\Delta_{BB}. \tag{10}$$

Substituting equations (8) and (10) into equation (1), and making the approximation $\ln X_B \approx -\eta\Delta_{BB}$, we obtain the bonding contribution to the free energy per particle at low temperature, and in the limit $\epsilon^*_{BB} \ll 1$:

$$\beta f_b = 1 - \ln(2\Delta_{AA}\eta) - (2\Delta_{AA}\eta)^{-\frac{1}{2}} - \frac{\Delta_{BB}\eta}{2}. \tag{11}$$

If the HS pressure is expanded in powers of the packing fraction, the total pressure becomes

$$\beta p v_s = \frac{1}{2}\left(\frac{\eta}{2\Delta_{AA}}\right)^{\frac{1}{2}} + (B_2 - \Delta_{BB})\frac{\eta^2}{2} + \frac{B_3}{6}\eta^3, \tag{12}$$

where $B_2/2 = 4$ and $B_3/6 = 10$ are, respectively, the second and third (dimensionless) virial coefficients of the reference HS fluid (see, e.g., [51]). The critical point is calculated using equations (31) and (32). Using definition (5) and the approximation $\Delta_{AA,c} \approx \frac{v_b}{v_s}\exp(\frac{1}{T^*_c})$

(justified because we are working the limit $\Delta_{AA} \to \infty$), we obtain, in the limit $\epsilon^*_{BB} \ll 1$, explicit expressions for the critical temperature and the critical density:

$$T^*_c = \frac{\epsilon^*_{BB}}{\ln\left(1 + \frac{B_2 v_s}{v_b}\right)}, \tag{13}$$

$$\eta_c = \frac{1}{2}\left(\frac{3}{B_3}\right)^{\frac{2}{5}} \exp\left[-\frac{\ln(1 + \frac{B_2 v_s}{v_b})}{5\epsilon^*_{BB}}\right]. \tag{14}$$

Therefore, when the limit of linear self-assembly is reached via the route ($\epsilon^*_{AB} = 0, \epsilon^*_{BB} \to 0$), a critical point is always present, with lower and lower critical density and temperature. This result appears similar to that obtained in [31], where the phase behaviour of a mixture of hard spheres with two and three identical bonding sites was investigated. Lowering the fraction of spheres with 3 bonding sites was seen to depress the critical density and temperature to vanishingly small values, nevertheless indicating that a critical point exists all the way to the linear self-assembly limit.

When $\epsilon^*_{AB} = 0, \epsilon^*_{BB} \to 0$, two chains, formed by AA bonds, are linked through a BB bond in a way reminiscent of fourfold X-junctions (see Figure 1a). This process is akin to the thermoreversible vulcanisation through molecular linkers discussed in [16] with the linkers replaced by BB bonds. As was pointed out in [16] the contribution of the X-junctions to the free energy is indistinguishable from the two-body attractions between monomers. Both contribute a term proportional to the density of monomers squared and the critical point driven by X-junctions described here is similar to the Θ point of polymer solutions. The bonding energy ϵ_{BB} that stabilises the X-junctions is a site-site interaction between monomers and a finite critical point follows as long as this interaction is attractive, $\epsilon_{BB} > 0$. By contrast, in the model considered in [16] the X-junction is repulsive (i.e., it has an energy higher than that of two separated chains) and there is no critical point at any finite temperature.

2. *Y-junction driven criticality:* $\epsilon^*_{BB} = 0$, $\epsilon^*_{AB} \to 0$

In the low-temperature limit, equation (8) holds, and when $\epsilon_{BB} = 0$, equation (3) gives

$$X_B = \frac{1}{1 + \gamma\eta^{\frac{1}{2}}}, \tag{15}$$

with $\gamma = 2\Delta_{AB}(2\Delta_{AA})^{-\frac{1}{2}}$. In the limit $\epsilon_{AB} \ll 1$ we must have $X_B \approx 1$ (i.e., no B sites are bonded), and consequently $\gamma\eta^{\frac{1}{2}} \ll 1$. Therefore, in this limit equation (15) can be approximated by

$$X_B = 1 - \gamma\eta^{\frac{1}{2}}. \tag{16}$$

Substituting equations (8) and (16) in equation (1) and making the approximation $\ln X_B \approx -\gamma\eta^{\frac{1}{2}}$, we obtain the bonding contribution to the free energy per particle at low temperature and in the limit $\epsilon_{AB} \to 0$:

$$\beta f^b = 1 - \ln(2\Delta_{AA}\eta) - \frac{1}{2}\gamma\eta^{\frac{1}{2}} - (2\Delta_{AA}\eta)^{-\frac{1}{2}}. \tag{17}$$

If the HS pressure is expanded in powers of the packing fraction, the total pressure becomes

$$\beta p v_s = \frac{1}{2}\left(\frac{\eta}{2\Delta_{AA}}\right)^{\frac{1}{2}} - \frac{\gamma}{4}\eta^{\frac{3}{2}} + \frac{B_2}{2}\eta^2, \tag{18}$$

where $B_2/2 = 4$ is, as before, the second coefficient of the (non-dimensionalised) virial expansion of the reference HS fluid. Equations (31) and (32) are used to find the critical point, yielding that it can only exist if $\epsilon^*_{AB} \geq \frac{1}{3}$. In the limit $\epsilon^*_{AB} \to \frac{1}{3}^+$, the critical temperature and the critical density are:

$$T^*_c = \frac{\epsilon^*_{AB} - \frac{1}{3}}{b}, \tag{19}$$

$$\eta_c = \exp\left(-\frac{\epsilon^*_{AB} b}{\epsilon^*_{AB} - \frac{1}{3}}\right), \tag{20}$$

with $b = \ln\left[2\left(\frac{B_2 v_s}{v_b}\right)^{\frac{2}{3}}\right]$ (notice that $b > 0$).

Consequently, on decreasing ϵ^*_{AB} a critical point of vanishingly small density and temperature is obtained up to $\epsilon^*_{AB} = \frac{1}{3}$. For $\epsilon^*_{AB} \leq \frac{1}{3}$, however, no vapour-liquid condensation is possible. In other words, unlike in the limit ($\epsilon^*_{AB} = 0, \epsilon^*_{BB} \to 0$), and contrary to the results of [31], the perturbation of linear self-assembly must have a minimum strength in order to generate a qualitatively different phase behaviour.

This result can be shown to be related to (in fact, it is almost the same as) that obtained in [16] for Y-junction-driven criticality. In that work, formation of a Y-junction was assumed to raise the energy of a linear ring (i.e., a ring of bonded particles without branching points) by ϵ_j (> 0); and formation of a chain (creation of two ends) from a linear ring was assumed to raise the energy by $2\epsilon_e$ (> 0). It was also shown that Y-junctions, apart from increasing

the energy, also increase the entropy of the system, in such a way that, if $\epsilon_j < \epsilon_e/3$, there is coexistence between an end-rich gas and a junction-rich liquid. The energy parameters of [16] are related to those of the present model by $2\epsilon_e = \epsilon_{AA}$ (since on creating two ends a AA bond is broken) and $\epsilon_j = -\epsilon_{AB} + \epsilon_{AA}/2$ (since on forming a Y-junction, one end and one AB bond are created). Given these relations, the condition $\epsilon_j < \epsilon_e/3$ of [16] is equivalent to $\epsilon^*_{AB} > \frac{1}{3}$ and the condition for 'repulsive' junctions ($\epsilon_j > 0$) becomes $\epsilon^*_{AB} < \frac{1}{2}$.

We may therefore interpret our result very precisely in terms of Y-junction formation. If $\epsilon^*_{AB} > \frac{1}{2}$, the formation of Y-junctions lowers the energy (relative to a chain-rich liquid phase), so we obtain the usual liquid phase (this range of parameters was not considered in [16]). If, on the other hand, $\frac{1}{3} < \epsilon^*_{AB} < \frac{1}{2}$, the increase in energy is compensated by the increase in the entropy of junction formation, and a junction-rich liquid phase is still possible. Finally, if $\epsilon^*_{AB} < \frac{1}{3}$ the energy cost of creating a junction is too large and condensation becomes impossible.

The results of both limits lend themselves to an interpretation in terms of the types of binding that can sustain a liquid phase: whereas any amount of BB binding energy (hence an arbitrarily low concentration of X-junctions) can stabilise liquid-vapour equilibrium, a minimal amount of AB energy (hence a finite concentration of Y-junctions) is needed for that purpose. In other words, Y-junctions are less effective than X-junctions at stabilising two-phase coexistence. This is in agreement with Tlusty and Safran's coexistence between a chain-end-rich vapour and a Y-junction-rich liquid and contrasts with their results for entropically stabilized X-junction-rich liquids [15–17].

IV. CONCLUSION

We have investigated the influence of strong directional, or bonding, interactions on the liquid-vapour critical point using a simple model and theory of self-assembly. Our ultimate goal is to develop a model that retains the symmetry of dipolar forces leading to association, and to relate the network structure of the dipolar fluid to its phase behaviour at low densities.

We have applied Wertheim's theory to patchy colloids with three sites: two of type A, with interaction strength ϵ_{AA}, and one of type B and strength ϵ_{BB}. Unlike sites also interact, with strength ϵ_{AB}. We have found generic first-order condensation with well-defined limits, as the BB or AB interaction strengths are varied. Some of these limits are relevant in the

context of polymer criticality, which in turn is relevant to the criticality of strongly dipolar fluids, since this is driven by network formation [15].

In our model we find self-assembled, polydisperse structures. However, polydispersity is thought to be irrelevant in the critical region of polymeric systems, so we expect our results to apply to monodisperse systems also. In the following we summarise them with emphasis on those for vanishing BB and AB interaction strengths.

1. In the limit of large ϵ_{AB} there is complete association of the B sites at the critical point, consistent with the formation of highly ramified clusters akin to hyperbranched polymers [40], the size of which grows as the bond gets stronger.

2. In the limit of large ϵ_{BB} there is a high degree of association of B sites in either phase; the vapour phase consists mostly of BB dimers, and the liquid phase of BB dimers connected by AA bonds.

3. In the limit of vanishing BB or AB interactions, fully-associated AA chains form with either AB or BB branches, depending on whether ϵ_{BB} or ϵ_{AB} vanishes, respectively. These are the relevant limits to strong-dipolar-fluid criticality. While a full investigation of the network properties will be left to future work, a number of conclusions may be drawn concerning the structure of the fluid in these limits, as will be discussed below.

When $\epsilon_{BB} = \epsilon_{AB} = 0$ we recover the limit of two identical patches of strength ϵ_{AA} [31–33]. This limit, however, turned out to be non-trivial: in systems where unlike sites do not interact (i.e., where $\epsilon_{AB} = 0$), the critical point exists all the way to $\epsilon_{BB}/\epsilon_{AA} = 0$. By contrast, when $\epsilon_{BB} = 0$, there is no critical point below a certain finite value of $\epsilon_{AB}/\epsilon_{AA}$. These findings were interpreted in terms of the formation of different network structures [16], and shown to be closely related to the network-based description of the criticality of strongly dipolar fluids [15].

Two AA chains are linked by one BB bond (X-junction) in systems with $\epsilon_{AB} = 0$ (X-junction), and by one AB bond (Y-junction) in systems with $\epsilon_{BB} = 0$. The vapour-liquid transition may then be viewed as the condensation of these junctions, and X-junctions are found to condense for any strength of the BB attraction (i.e., for any fraction of BB bonds), whereas condensation of the Y-junctions requires that the AB attraction be above a finite

threshold (i.e., there must be a finite fraction of AB bonds). We find that the critical point disappears above a certain threshold strength of the repulsive junction interaction ϵ_j, in agreement with the results of [16] for entropic junctions. Below that threshold the (entropically) junction-induced attraction is strong enough to drive a first-order phase separation, where the system separates into a low-density and a high-density phase. This entropic transition is driven by the large entropy of the high-junction-density phase that more than compensates the loss of translational entropy of the network [15]. The transition line terminates at a critical point. The critical temperature increases as the junction energy decreases and for attractive Y-junctions the high-density phase is stabilised by energetic and entropic junction contributions, the former becoming increasingly important as the junction energy decreases.

For fourfold junctions, we find that a junction-induced transition occurs as long as the junction is attractive, i.e., $-\epsilon_{BB} < 0$, vanishing when the strength of the BB bond vanishes. On the other hand, repulsive fourfold junctions induce an (entropic) attraction that is too weak to drive a phase separation, as found in [16].

The relation between network formation and the phase diagram of strongly dipolar fluids was proposed in [15] and shown to be consistent with the results of computer simulations in [19]. The interaction energy of two dipoles is lowest when the dipole moments are aligned head-to-tail. This implies that dipolar particles have a tendency to aggregate into linear chains. Yet it is important to realize that these chains can also branch, as shown in computer simulations of quasi-2D dipolar fluids [19]. The energy of the particle at the branching point is obviously higher than that of an interior chain particle, and can be calculated from electrostatics. Disregarding the long-range part of the dipole-dipole interactions, the system of branched dipolar chains can be mapped onto the model presented here, as was done originally by [15], and our predictions for the phase separation should apply. However, in view of the subtleties of the linear chain limit reported in this paper, and which had been overlooked in [15], a closer inspection of the strongly dipolar fluid model seems to be called for.

In future work we also plan to investigate (i) the effect of a continuously varying (effective) number of sites ('valence') and (ii) the interplay between percolation and phase coexistence, as gelation is also strongly affected by patchiness [37, 52].

Happy birthday JJ and all the best from the Lisbon team. We hope to see you back soon.

Acknowledgement

Financial support from the Foundation of the University of Lisbon and the Portuguese Foundation for Science and Technology (FCT) under Contracts nos. POCI/FIS/55592/2004 and POCTI/ISFL/2/618, is gratefully acknowledged.

Appendix

In order to find the critical point, we require the first and second derivatives of the pressure with respect to the packing fraction. From equation (6), the pressure comprises two contributions:

$$p = p_{HS} + p_b. \tag{21}$$

Here, p_{hs} is the pressure of the reference HS fluid, which we take to be given by the Carnahan-Starling formula [38],

$$\beta p_{HS} v_s = \frac{\eta\left(1+\eta+\eta^2-\eta^3\right)}{\left(1-\eta\right)^3}. \tag{22}$$

and p_b is the excess pressure due to bonding:

$$\beta p_b v_s = \eta^2\left[\left(\frac{2}{X_A}-1\right)\frac{\partial X_A}{\partial \eta}+\left(\frac{1}{X_A}-\frac{1}{2}\right)\frac{\partial X_B}{\partial \eta}\right]. \tag{23}$$

For completeness, and because it is used when computing the phase diagram, we also give the expression for the chemical potential:

$$\begin{aligned}
\beta\mu &= \beta\mu_{HS} + \beta\mu_b, && (24)\\
\beta\mu_{HS} &= \ln\eta + \frac{8\eta-9\eta^2+3\eta^3}{\left(1-\eta\right)^3}, && (25)\\
\beta\mu_b &= 2\ln X_A - X_A + \ln X_B - \frac{X_B}{2} + \frac{3}{2} \\
&\quad + \eta\left[\left(\frac{2}{X_A}-1\right)\frac{\partial X_A}{\partial \eta}+\left(\frac{1}{X_A}-\frac{1}{2}\right)\frac{\partial X_B}{\partial \eta}\right]. && (26)
\end{aligned}$$

Straightforward differentiation of equations (22) and (23) yields:

$$\begin{aligned}
\frac{\partial}{\partial\eta}\left(\beta p_{HS} v_s\right) &= \frac{1+4\eta+4\eta^2-4\eta^3+\eta^4}{\left(1-\eta\right)^4}, && (27)\\
\frac{\partial^2}{\partial\eta^2}\left(\beta p_{HS} v_s\right) &= \frac{8+20\eta+20\eta^2}{\left(1-\eta\right)^5}, && (28)\\
\frac{\partial}{\partial\eta}\left(\beta p_b v_s\right) &= \frac{2}{\eta}\left(\beta p_b v_s\right)
\end{aligned}$$

$$+\eta^2\left[-\frac{2}{X_A^2}\left(\frac{\partial X_A}{\partial\eta}\right)^2+\left(\frac{2}{X_A}-1\right)\frac{\partial^2 X_A}{\partial\eta^2}-\frac{1}{X_B^2}\left(\frac{\partial X_B}{\partial\eta}\right)^2+\left(\frac{1}{X_B}-\frac{1}{2}\right)\frac{\partial^2 X_B}{\partial\eta^2}\right], \quad (29)$$

$$\frac{\partial^2}{\partial\eta^2}(\beta p_b v_s) = -\frac{2}{\eta^2}(\beta p_b v_s)+\frac{2}{\eta}\frac{\partial}{\partial\eta}(\beta p_b v_s)$$
$$+2\eta\left[-\frac{2}{X_A^2}\left(\frac{\partial X_A}{\partial\eta}\right)^2+\left(\frac{2}{X_A}-1\right)\frac{\partial^2 X_A}{\partial\eta^2}-\frac{1}{X_B^2}\left(\frac{\partial X_B}{\partial\eta}\right)^2+\left(\frac{1}{X_B}-\frac{1}{2}\right)\frac{\partial^2 X_B}{\partial\eta^3}\right]$$
$$+\eta^2\left[\frac{4}{X_A^3}\left(\frac{\partial X_A}{\partial\eta}\right)^3-\frac{6}{X_A^2}\frac{\partial X_A}{\partial\eta}\frac{\partial^2 X_A}{\partial\eta^2}+\left(\frac{2}{X_A}-1\right)\frac{\partial^3 X_A}{\partial\eta^3}\right.$$
$$\left.+\frac{2}{X_B^3}\left(\frac{\partial X_B}{\partial\eta}\right)^3-\frac{3}{X_B^2}\frac{\partial X_B}{\partial\eta}\frac{\partial^2 X_B}{\partial\eta^2}+\left(\frac{1}{X_B}-\frac{1}{2}\right)\frac{\partial^3 X_B}{\partial\eta^3}\right]. \quad (30)$$

The critical point equations are then

$$\frac{\partial}{\partial\eta}(\beta p v_s) = \frac{\partial}{\partial\eta}(\beta p_{HS} v_s+\beta p_b v_s)=0, \quad (31)$$
$$\frac{\partial^2}{\partial\eta^2}(\beta p v_s) = \frac{\partial^2}{\partial\eta^2}(\beta p_{HS} v_s+\beta p_b v_s)=0. \quad (32)$$

It remains to calculate the first, second and third derivatives of X_A and X_B with respect to η. Differentiating the mass-action law equations (2) and (3), we obtain the following set of linear equations in the unknowns $\partial X_A/\partial\eta$, $\partial X_B/\partial\eta$:

$$a_{AA}\frac{\partial X_A}{\partial\eta}+a_{AB}\frac{\partial X_B}{\partial\eta}=b_A, \quad (33)$$
$$a_{BA}\frac{\partial X_A}{\partial\eta}+a_{BB}\frac{\partial X_B}{\partial\eta}=b_B, \quad (34)$$

with the solutions

$$\frac{\partial X_A}{\partial\eta} = \frac{a_{BB}b_A-a_{AB}b_B}{a_{AA}a_{BB}-a_{AB}a_{BA}}, \quad (35)$$
$$\frac{\partial X_B}{\partial\eta} = \frac{a_{AA}b_B-a_{BA}b_A}{a_{AA}a_{BB}-a_{AB}a_{BA}}. \quad (36)$$

where

$$a_{AA} = 4\eta\Delta_{AA}X_A+\eta\Delta_{AB}X_B+1, \quad (37)$$
$$a_{AB} = \eta\Delta_{AB}X_A, \quad (38)$$
$$a_{BA} = 2\eta\Delta_{AB}X_B, \quad (39)$$
$$a_{BB} = 2\eta\Delta_{BB}X_B+2\eta\Delta_{AB}X_A+1, \quad (40)$$
$$b_A = -2\Delta_{AA}X_A^2-\Delta_{AB}X_AX_B, \quad (41)$$
$$b_B = -\Delta_{BB}X_B^2-2\Delta_{AB}X_AX_B. \quad (42)$$

Analogous sets of linear equations for $\partial^2 X_A/\partial\eta^2$, $\partial^2 X_B/\partial\eta^2$ and $\partial^3 X_A/\partial\eta^3$, $\partial^3 X_B/\partial\eta^3$ can be derived by successive differentiation of equations (33) and (34), yielding:

$$a_{AA}\frac{\partial^2 X_A}{\partial\eta^2} + a_{AB}\frac{\partial^2 X_B}{\partial\eta^2} = c_A, \tag{43}$$

$$a_{BA}\frac{\partial^2 X_A}{\partial\eta^2} + a_{BB}\frac{\partial^2 X_B}{\partial\eta^2} = c_B, \tag{44}$$

$$a_{AA}\frac{\partial^3 X_A}{\partial\eta^3} + a_{AB}\frac{\partial^3 X_B}{\partial\eta^3} = d_A, \tag{45}$$

$$a_{BA}\frac{\partial^3 X_A}{\partial\eta^3} + a_{BB}\frac{\partial^3 X_B}{\partial\eta^3} = d_B, \tag{46}$$

with the solutions

$$\frac{\partial^2 X_A}{\partial\eta^2} = \frac{a_{BB}c_A - a_{AB}c_B}{a_{AA}a_{BB} - a_{AB}a_{BA}}, \tag{47}$$

$$\frac{\partial^2 X_B}{\partial\eta^2} = \frac{a_{AA}c_B - a_{BA}c_A}{a_{AA}a_{BB} - a_{AB}a_{BA}}, \tag{48}$$

$$\frac{\partial^3 X_A}{\partial\eta^3} = \frac{a_{BB}d_A - a_{AB}d_B}{a_{AA}a_{BB} - a_{AB}a_{BA}}, \tag{49}$$

$$\frac{\partial^3 X_B}{\partial\eta^3} = \frac{a_{AA}d_B - a_{BA}d_A}{a_{AA}a_{BB} - a_{AB}a_{BA}}, \tag{50}$$

where

$$c_A = \frac{\partial b_A}{\partial\eta} - \frac{\partial a_{AA}}{\partial\eta}\frac{\partial X_A}{\partial\eta} - \frac{\partial a_{AB}}{\partial\eta}\frac{\partial X_B}{\partial\eta}, \tag{51}$$

$$c_B = \frac{\partial b_B}{\partial\eta} - \frac{\partial a_{BA}}{\partial\eta}\frac{\partial X_A}{\partial\eta} - \frac{\partial a_{BB}}{\partial\eta}\frac{\partial X_B}{\partial\eta}, \tag{52}$$

$$d_A = \frac{\partial c_A}{\partial\eta} - \frac{\partial a_{AA}}{\partial\eta}\frac{\partial^2 X_A}{\partial\eta^2} - \frac{\partial a_{AB}}{\partial\eta}\frac{\partial^2 X_B}{\partial\eta^2}, \tag{53}$$

$$d_B = \frac{\partial c_B}{\partial\eta} - \frac{\partial a_{BA}}{\partial\eta}\frac{\partial^2 X_A}{\partial\eta^2} - \frac{\partial a_{BB}}{\partial\eta}\frac{\partial^2 X_B}{\partial\eta^2}. \tag{54}$$

The required derivatives of a_{ij}, b_i and c_i $(i, j = A, B)$ can be obtained from equations (37)–(42), (51) and (52); calculations are straightforward, but the resulting expressions are somewhat long, for which reason we do not present them here.

The critical point for given ϵ_{ij}, v^b_{ij} is then found by solving equations (2), (3), (31) and (32) simultaneously, for ρ, T, X_A and X_B, using NETLIB routine HYBRD.

[1] L. Verlet and J. J. Weis, Phys. Rev. A **5**, 939 (1972).

[2] J. J. Weis and D. Levesque, Phys. Rev. Lett. **71**, 2729 (1993).

[3] P. J. Camp, J. C. Shelley and G. N. Patey, Phys. Rev. Lett. **84**, 115 (2000).

[4] M. E. van Leeuwen and B. Smit, Phys. Rev. Lett. **71**, 3991 (1993).

[5] J. C. Shelley, G. N. Patey, D. Levesque and J. J. Weis, Phys. Rev. E **59**, 3065 (1999).

[6] S. C. McGrother and G. Jackson, Phys. Rev. Lett. **76**, 4183 (1996).

[7] G. Ganzenmüller and P. J. Camp, J. Chem. Phys. **126**, 191104 (2007).

[8] G. Ganzenmüller and P. J. Camp, J. Chem. Phys. **127**, 1545044 (2007).

[9] R. van Roij, Phys. Rev. Lett. **76**, 3348 (1996).

[10] R. P. Sear, Phys. Rev. Lett. **76**, 2310 (1996).

[11] M. A. Osipov, P. I. C. Teixeira and M. M. Telo da Gama, Phys. Rev. E **54**, 2597 (1996).

[12] J. M. Tavares, J. J. Weis and M. M. Telo da Gama, Phys. Rev. E **59**, 4388 (1999).

[13] K. Van Workum and J. F. Douglas, Phys. Rev. E **71**, 031502 (2005).

[14] J. M. Tavares, J. J. Weis and M. M. Telo da Gama, Phys. Rev. E **65**, 061201 (2002).

[15] T. Tlusty and S. A. Safran, Science **290**, 1328 (2000).

[16] A. G. Zilman and S. A. Safran, Phys. Rev. E **66**, 051107 (2002).

[17] A. Zilman, T. Tlusty and S. A. Safran, J. Phys.: Condens. Matter **15**, S57 (2003).

[18] J. P. Wittmer, P. van der Schoot, A. Milchev and J. L. Barrat, J. Chem. Phys. **113**, 6992 (2000).

[19] J. M. Tavares, J. J. Weis and M. M. Telo da Gama, Phys. Rev. E **73**, 041507 (2006).

[20] J. Dudowicz, K. F. Freed and J. F. Douglas, Phys. Rev. Lett. **92**, 045502 (2004).

[21] R. Hentschke, J. Bartke and F. Pesth, Phys. Rev. E **75** 011506 (2007).

[22] Y. V. Kalyuzhnyi, I. A. Protsykevytch and P. T. Cummings, Europhys. Lett. **80**, 56002 (2007).

[23] Yu. V. Kalyuzhnyi, I. A. Protsykevytch, G. Ganzenmüller and P. J. Camp, Europhys. Lett. **84**, 26001 (2008).

[24] M. S. Wertheim, J. Stat. Phys. **35**, 19 (1984).

[25] M. S. Wertheim, J. Stat. Phys. **35**, 35 (1984).

[26] A. van Blaaderen, Nature **439**, 545 (2006).

[27] P. I. C. Teixeira, J. M. Tavares and M. M. Telo da Gama, J. Phys.: Condens. Matter **12**, R411 (2000).

[28] V. F. Puntes, K. M. Krishnan and A. P. Alivisatos, Science **291**, 2115 2001.

[29] K. Butter, P. H. H. Bomans, P. M. Frederik, G. J. Vroege and A. P. Philipse, Nat. Mater. **2**,

88 (2003).

[30] M. Klokkenburg, C. Vonc, E. M. Claesson, J. D. Meeldijk, D. H.Erné and A. P. Philipse, J. Am. Chem. Soc. **126**, 16706 (2004).

[31] E. Bianchi, J. Largo, P. Tartaglia, E. Zaccarelli and F. Sciortino, Phys. Rev. Lett. **97**, 168301 (2006).

[32] G. Foffi and F. Sciortino, J. Phys. Chem. B **111**, 9702 (2007).

[33] E. Bianchi, P. Tartaglia, E. Zaccarelli and F. Sciortino, J. Chem. Phys. **128**, 144504 (2008).

[34] G. Jackson, W. G. Chapman and K. E. Gubbins, Molec. Phys. **65**, 1 (1988).

[35] L. G. MacDowell, M. Müller, C. Vega and K. Binder, J. Chem. Phys. **113**, 419 (2000).

[36] P. J. Flory, *Principles of Polymer Chemistry*, (Cornell University Press, Ithaca, 1981).

[37] F. Sciortino, E. Bianchi, J. F. Douglas and P. Tartaglia, J. Chem. Phys. **126**, 194903 (2007).

[38] N. F. Carnahan and K. E. Starling, J. Chem. Phys. **51**, 635 (1969).

[39] J. C. Wheeler and P. Pfeuty, J. Chem. Phys. **74**, 6415 (1981).

[40] M. Rubinstein and R. H. Colby, *Polymer Physics* (Oxford University Press, Oxford, 2003).

[41] M. J. Anselme, M. Gude and A. S. Teja, Fluid Phase Equilibria **57**, 347 (1990).

[42] E. D. Nikitin, P. A. Paylov and N. V. Bessonova, J. Chem. Thermodyn. **26**, 177 (1994).

[43] E. D. Nikitin, P. A. Pavlov and A. P. Popov, Fluid Phase Equilibria **141**, 155 (1997).

[44] B. Smit, S. Karaborni and J. I. Siepmann, J. Chem. Phys. **102**, 2126 (1995); **109**, 352 (1998).

[45] U.-J. Sheng, A. Z. Panagiotopoulos, S. K. Kumar and I. Szleifer, Macromolecules **27**, 100 (1994).

[46] N. B. Wilding, M. Müller and K. Binder, J. Chem. Phys. **105**, 802 (1996).

[47] M. S. Wertheim, J. Chem. Phys. **87**, 7323 (1987).

[48] B. Duplantier, J. Phys. France **43**, 911 (1982).

[49] B. Duplantier, J. Chem. Phys. **86**, 4233 1987.

[50] J. Hager and L. Schäfer, Phys. Rev. E **60**, 2071 (1999).

[51] J.-P. Hansen and I. R. McDonald, *Theory of Simple Liquids*, 2nd ed. (Academic Press, London, 1986).

[52] F. Sciortino, Eur. Phys. J. B **64**, 505 (2008).

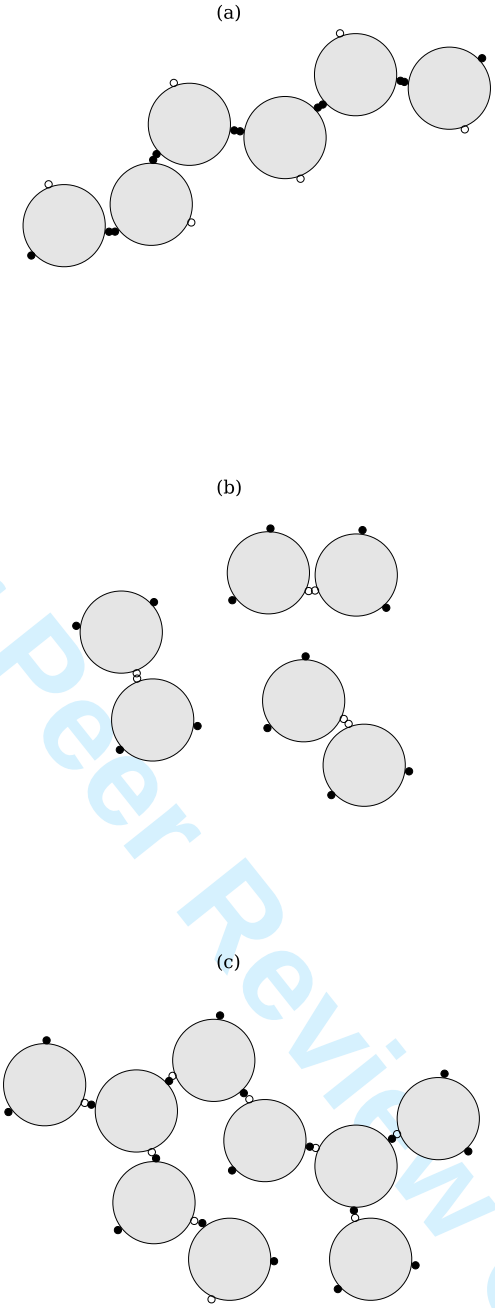

FIG. 1: Lowest-energy structures (without loops): (a) linear chains ($\epsilon_{AB} = \epsilon_{BB} = 0$, $\epsilon_{AA} \neq 0$), for which $X_A = 0$ and $X_B = 1$; (b) dimers ($\epsilon_{AA} = \epsilon_{AB} = 0$, $\epsilon_{BB} \neq 0$), for which $X_A = 1$ and $X_B = 0$; and (c) hyperbranched polymers ($\epsilon_{AA} = \epsilon_{BB} = 0$, $\epsilon_{AB} \neq 0$), for which $X_A = 0.5$ and $X_B = 0$. The small circles are the interaction sites: A (filled) and B (open).

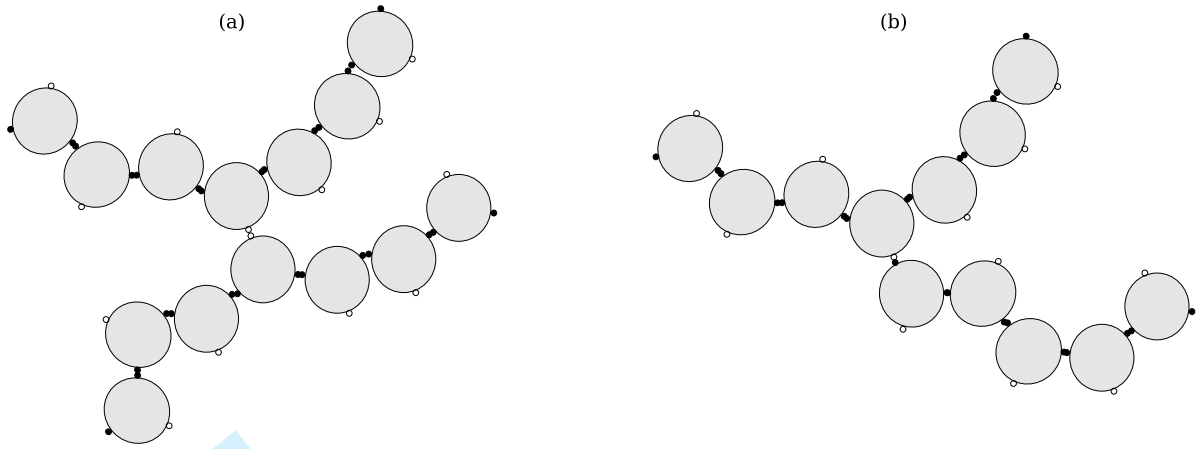

FIG. 2: (a) An X-junction; (b) a Y-junction.

(a)

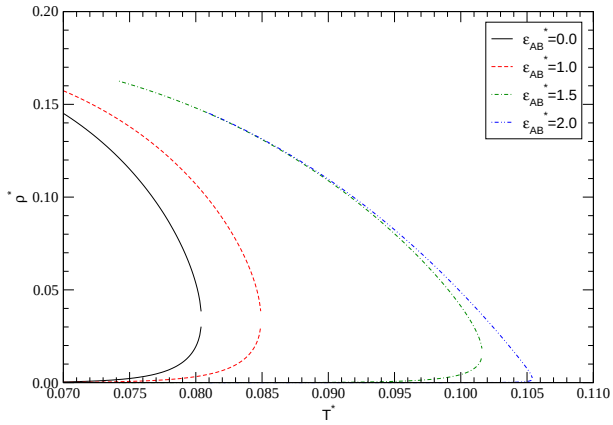

(b)

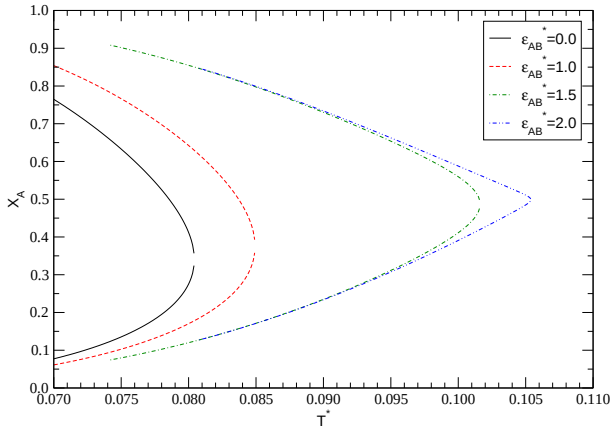

(c)

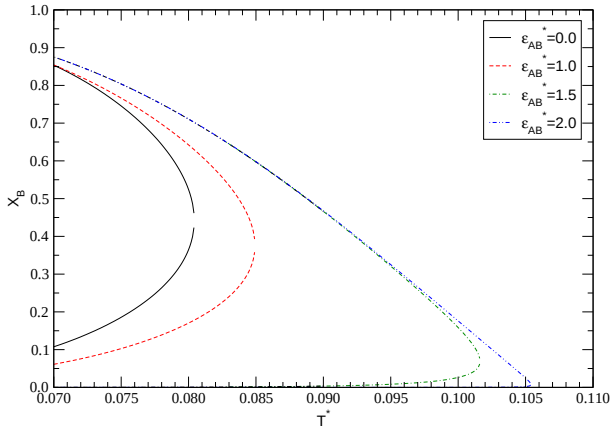

FIG. 3: (a) Temperature-density phase diagram, (b) fraction of unbonded A-sites, X_A, and (c) fraction of unbonded B-sites, X_B, for $\epsilon^*_{BB} = 1$ and variable ϵ^*_{AB}. In parts (b) and (c), the upper branches of the curves correspond to the vapour phase, the lower branches to the liquid phase.

(a)

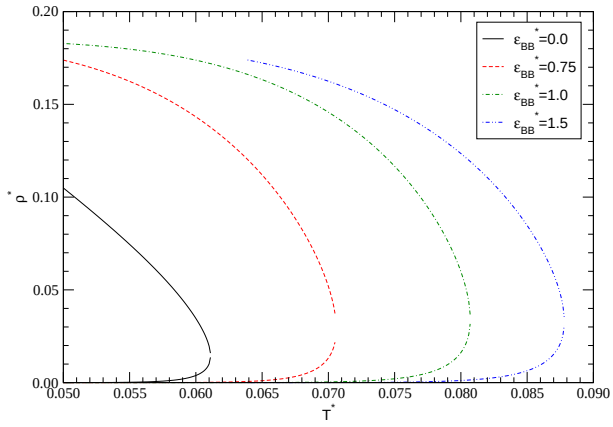

(b)

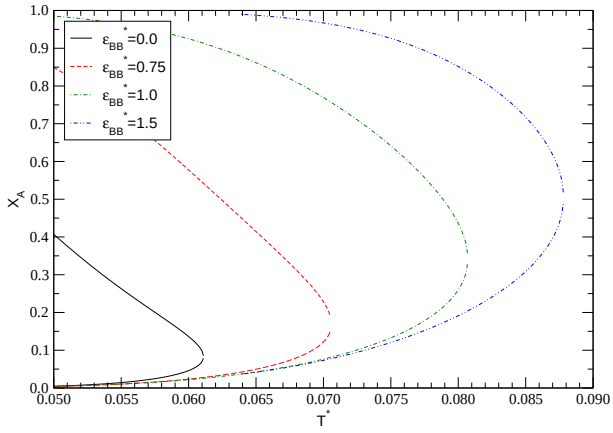

(c)

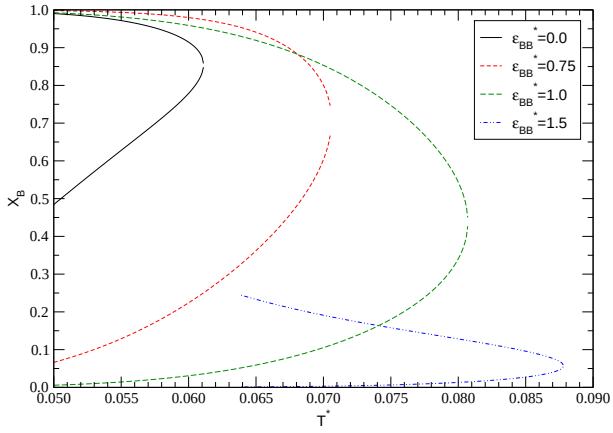

FIG. 4: (a) Temperature-density phase diagram, (b) fraction of unbonded A-sites, X_A, and (c) fraction of unbonded B-sites, X_B, for $\epsilon^*_{AB} = 0.75$ and variable ϵ^*_{BB}. In parts (b) and (c), the upper branches of the curves correspond to the vapour phase, the lower branches to the liquid phase.

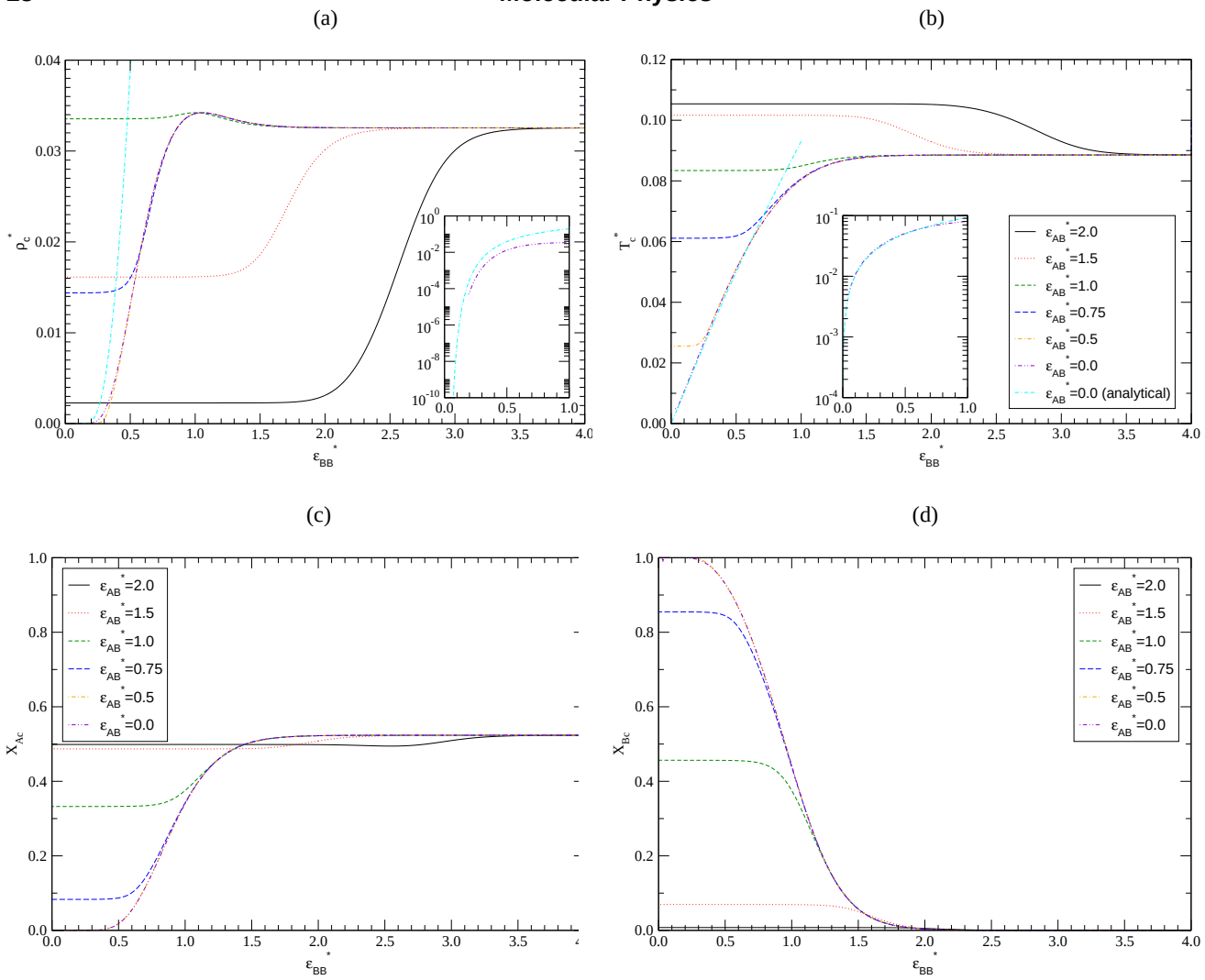

FIG. 5: Critical point *vs* ϵ_{BB} at different ϵ_{AB}: (a) critical density ρ_c^*; (b) critical temperature T_c^*; (c) X_A, the fraction of unbonded A sites; (d) X_B, the fraction of unbonded B sites. Symbols are the same for all panels. The insets in (a) and (b) compare the numerical and analytical results when $\epsilon_{AB} = 0$, $\epsilon_{BB} \to 0$.

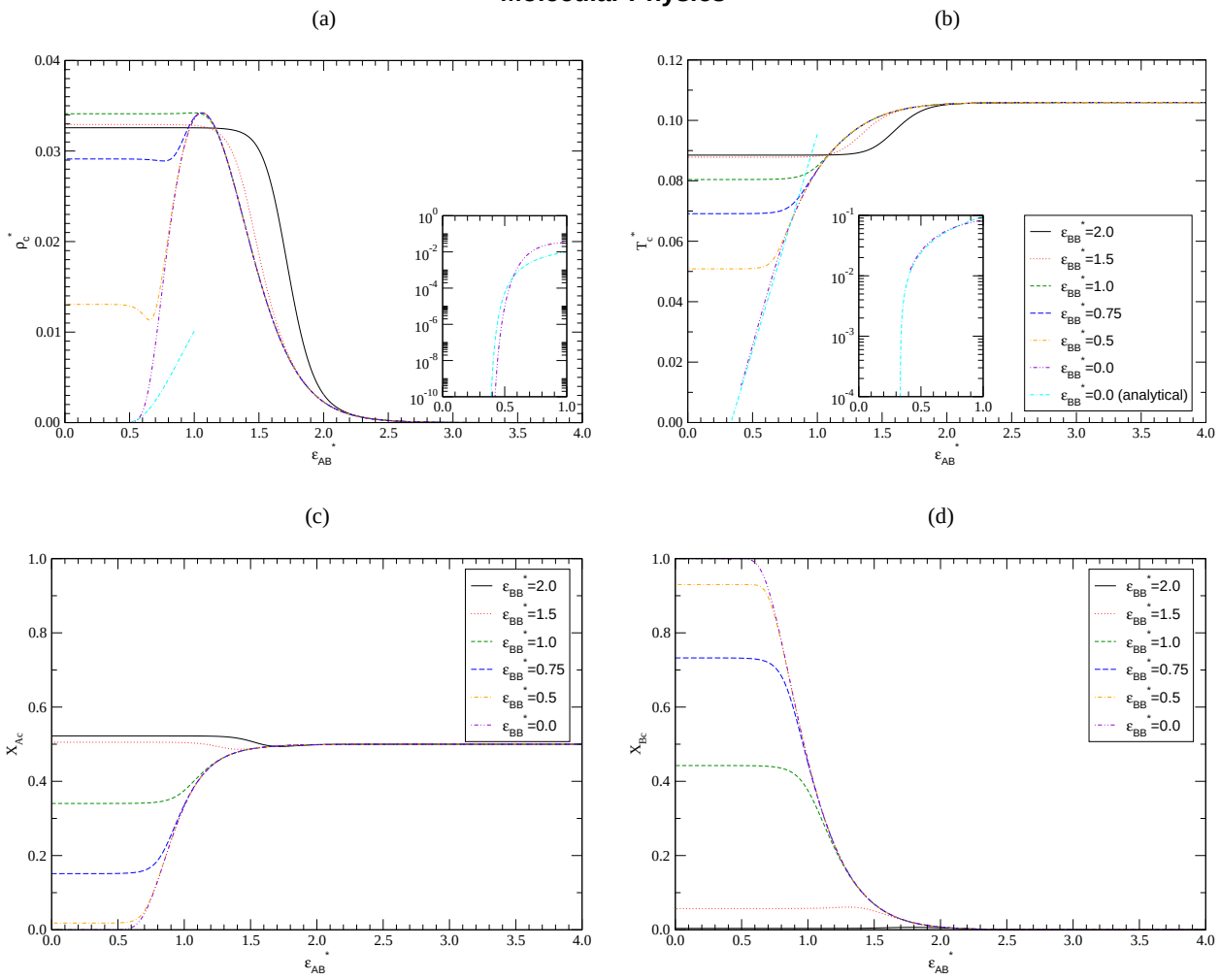

FIG. 6: Critical point *vs* ϵ_{AB} at different ϵ_{BB}: (a) critical density ρ_c^*; (b) critical temperature T_c^*; (c) X_A, the fraction of unbonded A sites; (d) X_B, the fraction of unbonded B sites. Symbols are the same for all panels. Note the non-monotonic behaviour of ρ_c^*, which is typical of self-assembling systems [35]. The insets in (a) and (b) compare the numerical and analytical results when $\epsilon_{BB} = 0$, $\epsilon_{AB} \to 0$.